PHYSICAL REVIEW B VOLUME 58, NUMBER 16 15 OCTOBER 1998-II

Optical polarization relaxation in $In_xGa_{1-x}As$-based quantum wells: Evidence of the interface symmetry-reduction effect

T. Guettler, A. L. C. Triques, L. Vervoort, R. Ferreira, Ph. Roussignol, and P. Voisin
Laboratoire de Physique de la Matière Condensée de l'Ecole Normale Supérieure, 24 rue Lhomond, F75005 Paris, France

D. Rondi
Laboratoire Central de Recherche, Thomson CSF, Domaine de Corbeville, F91400, Orsay, France

J. C. Harmand
France-Telecom-Centre National d'Etude des Télécommunications, 196 Avenue Henri Ravera, F92220 Bagneux, France

(Received 11 May 1998)

We report on the measurement of the spin dynamics in $In_xGa_{1-x}As$-$Al_xIn_{1-x}As$ and $In_xGa_{1-x}As$-InP multiquantum wells, using a fs pump and probe experiment. We observe a large difference in the polarization relaxation times, which confirms the recently predicted role of the interface symmetry reduction. [S0163-1829(98)51540-8]

It was recently realized that the local symmetry effects neglected in the classical envelope function theory (EFT) of semiconductor heterostructures may play a significant role in their electronic and optical properties.[1–3] A single semiconductor interface has the C_{2v} point-group symmetry, in which the in-plane directions (1,1,0) and (−1,1,0) are not equivalent. In a nominally square quantum well (QW), this asymmetry may be compensated or not, depending on the degree of symmetry of the consecutive interfaces. This leads to the overall D_{2d} or C_{2v} symmetries. The EFT Hamiltonian possesses at least the C_{4v} symmetry, and is necessarily incorrect from this point of view. In general, the consequences of EFT oversymmetry are weak in heterostructures where the hosts materials share a common atom (CA-QW's), like GaAs-(AlGa)As or (GaIn)As-(AlIn)As. On the other hand, a huge ''forbidden'' optical anisotropy is usually observed in systems where the well and barrier have different anions and cations (NCA-QW's), like (InGa)As-InP (Ref. 1) or InAs-GaSb. The correct symmetries can be restored in the envelope function approach either by generalizing the interface boundary conditions[2] or by a perturbative approach known as the H_{BF} model.[3] These theories are actually equivalent, and explain the in-plane anisotropy by a coupling of the heavy- and light-hole states at the zone center.

A remarkable consequence of the symmetry reduction is that the interplay of zone-center mixing and k_t-dependent mixing due to the Luttinger Hamiltonian leads to a large lifting of the parity degeneracy of the valence subband dispersions.[4] These effects are most conveniently calculated in the perturbative framework of the H_{BF} model, where interface perturbation matrix elements and in-plane motion are treated on the same foot, following the ''truncated basis'' method.[5] It follows that spin-relaxation phenomena[6] must be strongly affected by the symmetry of interfaces: indeed, in the D'yakonov-Perel (DP) mechanism,[7] the relaxation is tightly linked to the lifting of parity degeneracy. Calculations for $In_xGa_{1-x}As$-InP QW's (Ref. 4) show that the main process in the valence band becomes the DP mechanism, and is orders of magnitude faster than the Elliot-Yafet-like mechanism (spin-flip collisions between degenerate states having the mixed heavy- and light-hole character) previously considered in the literature.[8,9] The extension of these calculations to the conduction band[10] shows that interface inversion asymmetry plays in this case a role quantitatively similar to that of the bulk inversion asymmetry and structure inversion asymmetry (respectively, BIA and SIA).

The purpose of this paper is to present an experimental comparison of spin dynamics measured in CA- and NCA-QW's namely, (InGa)As-(AlIn)As and (InGa)As-InP QW's, having equivalent parameters and quality. Both the raw data and their interpretation through simple rate equations reveal the essential role of interface symmetries in these phenomena.

The two samples reported here are a $In_xGa_{1-x}As$ (113 Å)-InP (100 Å) 50-period multiquantum well (MQW) (S1) grown by metal-organic chemical-vapor deposition and a $In_xGa_{1-x}As$ (100 Å)-$Al_xIn_{1-x}As$ (70 Å) 50-period MQW (S2) grown by conventional molecular beam epitaxy (MBE). These state-of-the-art lattice-matched MQWs form the intrinsic region of pin diodes. They were characterized by various optical experiments including polarization resolved transmission, photoluminescence (PL), photoluminescence excitation (PLE), and photocurrent (PC) spectroscopy. Spin dynamics was investigated by a pump and probe absorption-saturation experiment using a tunable fs laser consisting of a parametric oscillator pumped by a Ti:Sapphire laser.

Relevant spectroscopic information is summarized on Fig. 1 that shows the PLE spectra (together with calculated band-to-band absorption) obtained in S2 (a) and S1 (b) with a low-power dc source. Trace (c) shows the absorption in S1 measured with the fs laser. The broadening of optical transitions observed in the latter case can be entirely attributed to the spectral width (10 meV) of the pulses, in the sense that convolution of curve (b) with the measured pulse spectrum [curve (d) in Fig. 1] exactly reproduces curve (c). However, significant bleaching of the excitons due to the strong excitation may occur simultaneously. Measurement of the optical anisotropy[1,11] shows a relative absorption difference between

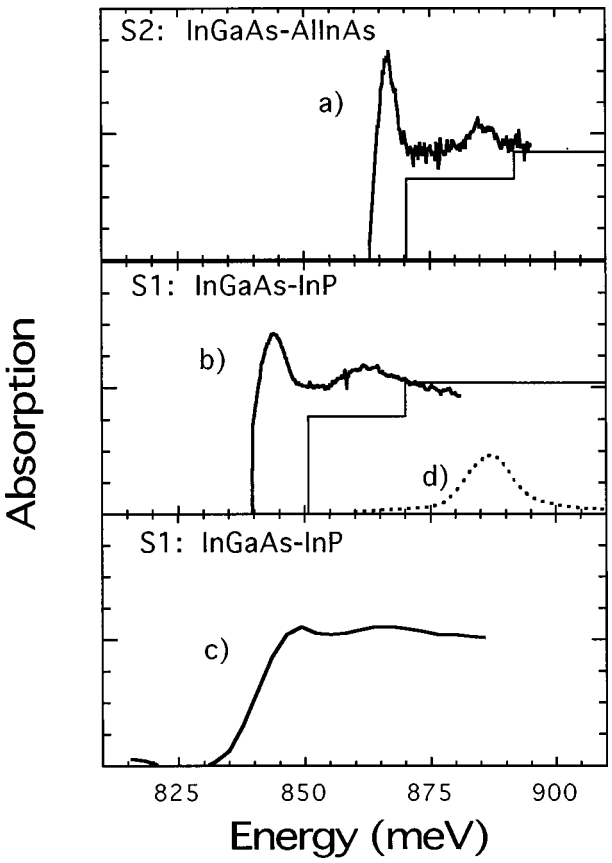

FIG. 1. Low-temperature (2 K) photoluminescence excitation spectra of samples S2 [trace (a)] and S1 [trace (b)] using a low-power dc optical source. Trace (c) shows the optical absorption obtained in S1 using the fs laser, which has the pulse line shape illustrated by trace (d). Convolution of (b) and (d) gives a nearly perfect fit of (c).

the $(-1,1,0)$ and $(1,1,0)$ directions of 10% in the case of S1, in the spectral range between the first heavy- and light-hole transitions $H1$-$E1$ and $L1$-$E1$. Somewhat surprisingly, S2 is not perfectly isotropic but shows anisotropy about one order of magnitude smaller than S1. The 20-meV band-gap difference is mainly due to the difference in conduction-band offsets, 500 meV in S2 and 245 meV in S1. Due to compensation between the well width difference and offset difference, the valence-band structures of the two samples are nearly the same. Stark effect measurements by PC confirm the value of the sample parameters. The dispersion of the Stark shifts is negligible, which puts an upper limit to residual doping in the few 10^{15} cm^{-3} range for both samples.

The low-temperature (2 K) absorption-saturation experiment is sketched in the inset of Fig. 2. Polarization resolved experiments are subjected to a number of artifacts associated with cryostat windows, imperfect λ/4 plates, etc. These experimental details have been quite carefully counterchecked in the present experiments. A σ_+ circularly polarized pump pulse (pulse duration 130 fs) is focused on the sample, at nearly normal incidence. It saturates the absorption for this polarization at zero time delay, and then spin relaxation decreases the saturation of σ_+ absorption, while increasing the saturation of the opposite polarization σ_-. This is probed by measuring the transmission of the delayed probe pulse that is much weaker and tightly focused in the middle of the

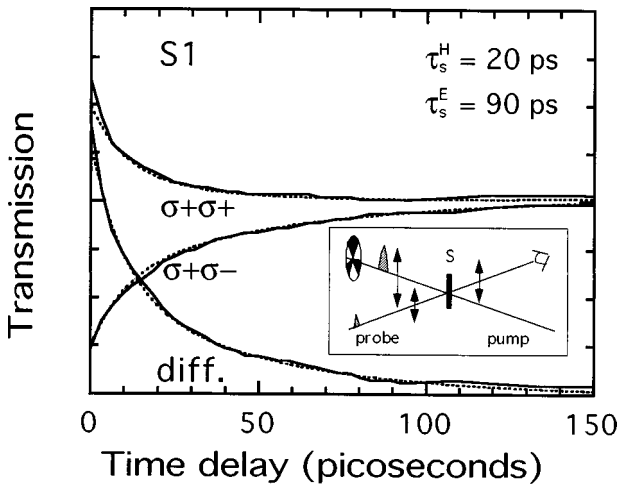

FIG. 2. Optical saturation signals versus pump-probe delay in the $\sigma_+\sigma_+$, $\sigma_+\sigma_-$, and differential (diff) configurations (solid lines) for the NCA-QW S1, and corresponding calculations (dotted lines), with the spin-relaxation times as indicated. We use $\beta=0.17$, $\alpha_{inc}=0.3$, $\tau_{inc}=100$ ps, and $\tau_{dec}=1$ ns. The inset shows a scheme of the experimental setup.

pumped area. The interval between two pulses is 12 ns, which turns out to be much longer than any relaxation time involved in these samples. The pump is chopped at low frequency (225 Hz), and the time integrated probe transmission is measured with conventional lock-in detection. By rotating a λ/4 retardation plate, one can also measure directly the difference between the σ_+ and σ_- saturation signals. The three signals [$\sigma_+\sigma_+$ and $\sigma_+\sigma_-$ transmissions (I_+ and I_-), and their difference] obtained at zero detuning (i.e., with the pulse peak wavelength resonant with the sample band gaps, 844 meV in S1 and 867 meV in S2) are shown in Figs. 2 and 3, together with theoretical fits discussed in the following.

The first and most significant result of these investigations is the order-of-magnitude difference in the time scales involved in the two samples, despite the remarkable similarity of the PLE spectra in Fig. 1. We have also investigated another $In_xGa_{1-x}As$-InP sample S3, having similar parameters and quality, but grown by the gas-source MBE technique.

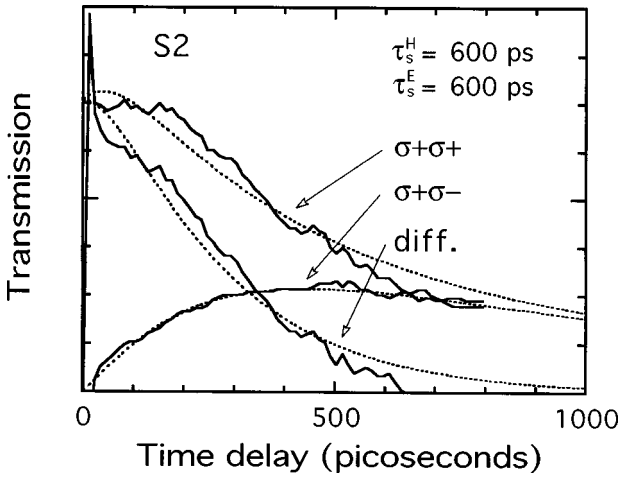

FIG. 3. Same as Fig. 2, but for the CA-QW S2. We use $\beta=0$, $\alpha_{inc}=0.3$, $\tau_{inc}=100$ ps, and $\tau_{dec}=1$ nm. Note that the time scale differs by nearly an order of magnitude from that of Fig. 1.

Results in S1 and S3 are equivalent, which rules out the growth technique as a main cause. These observations agree qualitatively with the theoretical prediction of short spin-relaxation times in NCA-QW's,[4,10] and we shall further on discuss and discard alternative explanations. It is noteworthy that our observation of an anomalously short relaxation at 2 K in $In_xGa_{1-x}As$-InP QW's is perfectly consistent with previous room-temperature investigations of GaAs-$Al_xGa_{1-x}As$ (Ref. 12) and $In_xGa_{1-x}As$-InP (Ref. 13) QW's.

In contrast with the simplicity of the experimental results, the physics of spin relaxation is extremely involved because many relaxation phenomena compete with spin-flip mechanisms. In order to go further in the analysis of these data, it is necessary to make several simplifying assumptions, the hierarchy of which may change from one sample to another. The most delicate assumption here is to neglect the excitonic interaction, which is supported by exciton screening in the strong excitation regime used in the present experiment. Also, in view of Fig. 1(c), this seems definitely a better approximation than the opposite limit of discrete exciton states, which would prevail in high-quality GaAs-$Al_xGa_{1-x}As$ QW's at low excitation.[14,15] Yet, we always stay in the weak saturation regime where the fraction of occupied states remains smaller than 0.1. This is proved experimentally by the fact that the saturation signal is a small fraction (<0.1) of the transmitted probe (the absorption is 50%, so absorption and transmission are equivalent). Also, we make the common assumption that the spin-conserving collision rate is much larger than the spin-flip rate. In practice, this means that the initial coherence of the electron and hole populations in k_t space is destroyed in a time comparable with the pulse duration. Also, the evolution from the initial nonthermal carrier distribution to a Maxwell distribution of hot carriers occurs in a similarly short time scale. Conversely, cooling of this population down to the lattice temperature, which implies interaction with acoustical phonons, occurs on a longer time scale (typically 100 ps), shorter than spin relaxation in S2, and longer in S1. We insist that the spin-conserving collision times in both samples are expected to be similar. With all these approximations in mind, one can describe the measured signals I_+ and I_- with very simple equations:

$$I_+ = [(f_{E_+} + f_{H_+}) + \beta f_{E_-}](1 - \alpha_{\rm inc} e^{-t/\tau_{\rm inc}}) e^{-t/\tau_{\rm dec}}$$

$$I_- = [(f_{E_-} + f_{H_-}) + \beta f_{E_+}](1 - \alpha_{\rm inc} e^{-t/\tau_{\rm inc}}) e^{-t/\tau_{\rm dec}},$$

where

$$f_{H_\pm} = 0.5(1 \pm e^{-2t/\tau_s^H}),$$

$$f_{E_\pm} = 0.5(1+\beta) \pm 0.5(1-\beta) e^{-2t/\tau_s^E}.$$

β is a creation factor measuring the initial polarization (see below), and τ_s^E and τ_s^H the spin-flip times of electrons and heavy holes (averaged over the actual energy distribution). $\tau_{\rm dec}$ is a time characteristic of the population decay (this includes thermalization in bound states or band tails, and recombination) and $\tau_{\rm inc}$ a time characteristic of phenomena contributing to increase the saturation signal by a coefficient $(1-\alpha_{\rm inc})^{-1}$, such as the thermalization of carriers created in the upper energy edge of the pulse and redistributing closer to the pulse maximum. For instance, evolution from the initial nonthermal distribution to a cold Boltzmann distribution gives $\alpha_{\rm inc} = 0.3$. On the one hand, these simple exponentials form a very crude description of underlying physics, but on the other hand, they are the simplest approach to phenomena that necessarily occur during the investigated time scale. Fortunately, the signatures of the various contributions differ, which allows a rapid convergence of the fitting procedure. The need for the factor β arises from the clear jump of the $\sigma_+\sigma_-$ signal in Fig. 2, which corresponds to finite depolarization at $t=0$. There are different contributions to β: the first one is the geometry of the experiment, with laser beams not exactly normal to the sample surface. The small in-plane projection creates depolarized carriers. Numerical estimates lead to very small β (in the percent range), which depends neither on the sample nor on the detuning. The second contribution comes from the heavy- and light-hole mixing at $k_t = 0$ which must exist in the NCA sample S1 in order to explain the 10% anisotropy of the optical absorption under linear polarization. This sample-dependent contribution is small in the present case, less than a percent in S1 and of course zero in S2. The contribution dominating the actual β is the most trivial one, that is the energetic overlap of the pulse with the light-hole transition, which creates electrons in the wrong polarization. We have estimated the corresponding β from the PLE spectra and measured pulse line shape shown in Fig. 1. We find $\beta = 0.14$ in S1, and $\beta < 0.03$ in S2, which are in agreement with the fitted values (0.17 and zero, respectively).

The data in Fig. 2 clearly involve two distinct time constants, a short one (10 ps), which we attribute to hole spin relaxation, and a longer one (45 ps) associated with electrons. Theoretical curves using a single relaxation time yield a very poor fit. Population redistribution does not affect significantly the relaxation curves in this case, in the sense that the finite $\alpha_{\rm inc} = 0.3$ and $\tau_{\rm inc} = 100$ ps simply improve the quality of the fit at long delays. The fitted values are $\tau_s^E = 90$ ps and $\tau_s^H = 20$ ps. On the other hand, the data corresponding to S2 (Fig. 3) are best fitted with equivalent electron ad heavy-hole spin-relaxation times $\tau_s^E = \tau_s^H = 600$ ps. Relaxation curves are obviously affected by the population redistribution, since the larger time scale allows for more complete carrier thermalization, and partial recombination. It is noteworthy that ''blind'' fitting leads to nearly equal $\alpha_{\rm inc}$ and $\tau_{\rm inc}$ in the two samples. Furthermore, the value of $\tau_{\rm inc}$ is in the expected range for a hot carrier thermalization time. Detailed discussion of the evolution of these results with increasing detuning δ is out of the scope of this paper, but the general trends (investigated from $\delta = -3$ meV up to 6 meV) basically support our analysis: the β factor in S1 and S2 increases dramatically when moving the pulse towards higher energies, population redistribution plays a more prominent role, while spin-relaxation times decrease slowly, both in S1 and S2. Conversely, negative detuning of a few meV's tends to increase the spin-relaxation time, as carriers closer to the zone center are probed.

Calculations using the H_{BF} model allow at least partial comparison of these results with theory. When spin degeneracy is lifted, the D'yakonov-Perel mechanism usually dominates spin relaxation. It is described by the simple formula $1/\tau_{DP} = 0.5\tau_p(\Delta E/\hbar)^2$, where ΔE is the spin splitting

and τ_p a momentum relaxation time. This relation shows that the shorter the collision time, the longer the spin-flip time. τ_p is governed by the spin-conserving collisions, and to a good approximation, $m_E\tau_p^E = m_H\tau_p^H$, where $m_{E,H}$ is the in-plane mass of the corresponding particle. For S1, our band-structure calculations using values of the interface potentials fitting the observed optical anisotropy give a conduction-band spin splitting (0.1 meV for $k_t = 0.01$ Å^{-1}) an order of magnitude smaller than the heavy-hole one (1 meV for the same value of k_t). Both spin splittings are linear in k_t. Although this calculation does not take into account the BIA contribution to electron spin splitting and therefore overestimates the electron spin-flip time, the qualitative trends and the orders of magnitude are in fair agreement with our observations. Using $\tau_p^H = 100$ fs, we indeed deduce $\tau_s^H = 30$ ps and $\tau_s^E = 300$ ps for $k_t = 0.005$ Å^{-1}, which corresponds to the average k_t for the zero detuning configuration. Including the BIA contribution to electron spin splitting would bring τ_s^E very close to the observed 90 ps. Conversely, for a CA-QW without band-bending, the hole spin relaxation time should be governed by the slow Elliot-Yafet mechanism[8,9] and the electron relaxation time by the DP mechanism associated with the sole BIA contribution.[16,17] Hole spin relaxation time should be rather large, and electron spin-relaxation time significantly longer than in an otherwise equivalent NCA-QW. This clearly corresponds to our observations in S2.

Although what precedes clearly shows that the predictions of the H_{BF} model are in agreement with the observations, it is interesting to go further and discard other possible explanations based on existing differences in confinement energies, scattering center density, and competition with other spin-relaxation mechanisms. As already mentioned, due to larger conduction-band offset, S2 has a much larger electron confinement energy (53 meV) than S1 (36 meV). The electron spin-flip rate due to $Ga_xIn_{1-x}As$ BIA should increase linearly[16,17] with increasing electron confinement energy, while we observe the opposite trend. Similarly, the DP spin-flip time should increase with decreasing τ_p, which means that the better the sample, the shorter the spin-flip time. Again, we observe the opposite trend, with the better quality S2 (using exciton linewidth as a measure) showing longer spin relaxation. As far as valence band is concerned, we have already mentioned that the $H1$, $L1$, and $H2$ levels are nearly at the same energies in both samples. The Elliot-Yafet mechanism that would prevail in the absence of H_{BF}-related spin splitting would lead to the prediction of equivalent hole spin relaxation in both samples. Hence, all the qualitative dependences deduced from classical analysis are opposite to the observed trends.

In conclusion, a huge difference was observed in the spin dynamics of a CA-QW and a NCA-Qw having similar parameters and overall quality. This experimental fact supports the role of the interface symmetry-reduction effect, which was until recently neglected in the envelope function theory. The results yield a fair agreement with the predictions of the H_{BF} model.

We thank Dr. O. Krebs for a number of fruitful discussions. A.L.C.T. was supported by FAPESP (São Paulo, Brazil). L.V. was supported by NATO and DEPHY(ENS).

[1] O. Krebs, W. Seidel, J. P. André, D. Bertho, C. Jouanin, and P. Voisin, Semicond. Sci. Technol. **12**, 938 (1997).
[2] E. Ivchenko, A-Yu Kaminski, and U. Rössler, Phys. Rev. B **54**, 5852 (1996).
[3] O. Krebs and P. Voisin, Phys. Rev. Lett. **77**, 1829 (1996).
[4] L. Vervoort, R. Ferreira, and P. Voisin, Phys. Rev. B **56**, R12 744 (1997).
[5] G. Bastard and J. A. Brum, IEEE J. Quantum Electron. **QE22**, 1625 (1986).
[6] For a review, see L. Sham, J. Phys.: Condens. Matter **A51**, (1993) and references therein.
[7] M. I. D'yakonov and V. I. Perel, Zh. Eksp. Teor. Fiz. **60**, 1954 (1971) [Sov. Phys. JETP **33**, 1053 (1971)]; Fiz. Tverd. Tela (Leningrad) **13**, 3581 (1971) [Sov. Phys. Solid State **13**, 3023 (1972)].
[8] T. Uenoyama and L. J. Sham, Phys. Rev. Lett. **64**, 3070 (1990).
[9] R. Ferreira and G. Bastard, Phys. Rev. B **43**, 9687 (1991).
[10] L. Vervoort, R. Ferreira, and P. Voisin (unpublished).
[11] O. Krebs *et al.*, Physica E **2**, 59 (1998).
[12] A. Tackeuchi, Y. Nishikawa, and O. Wada, Appl. Phys. Lett. **68**, 797 (1996).
[13] A. Tackeuchi, O. Wada, and Y. Nishikawa, Appl. Phys. Lett. **70**, 1131 (1997).
[14] A. Vinattieri, J. Shah, T. C. Damen, D. S. Kim, L. N. Pfeiffer, M. Z. Maialle, and L. J. Sham, Phys. Rev. B **50**, 10868 (1994).
[15] L. Muñoz, E. Pérez, L. Viña, and K. Ploog, Phys. Rev. B **51**, 4247 (1995).
[16] M. I. D'yakonov and V. Yu. Kochorovskii, Sov. Phys. Semicond. **20**, 110 (1086).
[17] G. Bastard and R. Ferreira, Surf. Sci. **267**, 335 (1992).